

NASA/CR—2002-210808



# Study Task for Determining the Effects of Boost-Phase Environments on Densified Propellants Thermal Conditions for Expendable Launch Vehicles

Mark S. Haberbusch  
Sierra Lobo, Inc., Freemont, Ohio

Prepared under Contract NAS3-C-73676-J

National Aeronautics and  
Space Administration

Glenn Research Center

---

April 2002

## Acknowledgments

The author wishes to acknowledge and thank Mr. Michael L. Meyer of NASA Glenn Research Center for his technical guidance throughout this research program. His drive for implementing advanced technologies into flight systems is refreshing and greatly appreciated. The author also wishes to thank Mr. Michael Carney and Ms. Laurie Walls of the NASA Kennedy Space Center ELV Launch Services Directorate. Their interest and support for this study is deeply appreciated. The author also acknowledges Mr. Jay Risberg of Lockheed Martin Astronautics, Denver, Colorado. Mr. Risberg has supplied valuable Atlas/Centaur flight data which has been extremely useful for conducting this applied research. The author wants to thank Mr. Robert Stochl of Sierra Lobo for his thorough review of the research. His unprecedented experience in cryogenic systems is greatly appreciated. This research was conducted under NASA contract number C-73676-J and was administered out of the NASA Glenn Research Center (formally the NASA Lewis Research Center). Data exchange between Sierra Lobo and Lockheed Martin Astronautics was protected under a Non-Disclosure Agreement.

Available from

NASA Center for Aerospace Information  
7121 Standard Drive  
Hanover, MD 21076

National Technical Information Service  
5285 Port Royal Road  
Springfield, VA 22100

Available electronically at <http://gltrs.grc.nasa.gov/GLTRS>

# **Study Task for Determining the Effects of Boost-Phase Environments on Densified Propellants Thermal Conditions for Expendable Launch Vehicles**

Mark S. Haberbusch  
Sierra Lobo, Inc.  
Freemont, Ohio 43420

## **Introduction**

Next generation aerospace vehicles will require new technologies to meet the performance goals demanded in today's highly-competitive and resource-limited environment. These performance goals are being driven by both government payloads and missions and the rapidly expanding commercial satellite market. Potential performance improving technologies vary widely in development maturity. However, the risks and payoffs associated with bringing them to commercial fruition are equally wide ranging.

One technology with tremendous potential, that has graduated far beyond the laboratory and is poised for commercial exploitation, is propellant densification. In this context, propellant densification refers to cryogenic propellants such as hydrogen or oxygen that have been cooled below their normal boiling point temperature but still remain in their liquid state. The primary advantages of densified propellants over their normal boiling point counterparts relates to the increase in propellant density and the greater sensible cooling capacity. Figures 1 and 2 show the increase in density and cooling capacity for hydrogen and oxygen respectively, as a function of liquid temperature.

## **Benefits of Densified Propellants**

There are many benefits to using densified propellants on launch and space vehicles. The increase in propellant density translates into smaller propellant tanks, which result in lower take-off weight and larger vehicle payload capacities. The increased subcooling of densified propellants allows lower system operating pressures in propellant tanks, which extends tank life in reusable systems thus lowering recurring costs and reducing life-cycle costs. Lower system operating pressures for expendable launch vehicles results in lower pressurant gas requirements. The increased density also lowers turbomachinery rotational speeds, which increases reliability and safety and reduces life-cycle costs for reusable systems. The increased cooling capability provides a vital heat sink for leading edges and shock wave regions subjected to aerodynamic heating as well as for rocket or rocket based combined cycle (RBCC) engine combustion chambers and nozzles.

There have been many studies showing the benefits of using densified propellants on aerospace vehicles. Several of these studies have quantified the potential benefit of using densified propellants in terms of increased payload to orbit for several types of vehicles. McNelis shows a 4.9 percent increase in payload to Low Earth Orbit using 25 °R hydrogen and 140 °R oxygen on a cryogenic upper stage similar to the Atlas/Centaur or Delta III class vehicle (ref. 1). Friedlander reports that an orbital transfer vehicle can increase its payload capability from LEO to GEO by 7 percent using triple point hydrogen (ref. 2). Fazah examined the use of densified propellants on the Space Transportation System (STS) and found the payload to LEO could be increased by 17.5 percent by using densified oxygen at 132 °R and hydrogen at 28.5 °R (ref. 3). It was also reported that the National Aerospace Plane single-stage-to-orbit vehicle gross-take-off-weight would be reduced by as much as 26 percent using slush hydrogen as the fuel (ref. 4). Slush hydrogen is a mixture of liquid and solid hydrogen. The thermodynamics of slush hydrogen are not addressed in this study.

## Thermodynamic Study

Even though densified cryogenic propellant technology for launch vehicles has been shown many times to be a significant benefit to the launch industry, the concept has not been embraced. The main reason for this is the industry's resistance to change. Rocket vehicle and rocket engine designers have been working with normal boiling propellants since rockets were first invented.

A quote from Huzel and Huang summarizes the importance of choosing the propellants before the design: "The selection of the propellants is one of the most important steps in the design of an engine" (ref. 5). Once a designer fixes the propellant temperature then all of the hardware is designed around it.

This resistance to change is anchored by the perceived risk of implementing new or different technologies. Insufficient knowledge or the insufficient dissemination of knowledge is the primary driver behind perceived risk. One perceived risk of implementing densified propellant technology in staged rockets is that of over expansion of the liquid. Upper stages, especially, have been perceived risky, since environmental heating during the boost-phase may cause liquid over expansion. Liquid over expansion would cause the ullage volume to decrease below the minimum allowable volume for tank pressure control.

The thermodynamic study presented here directly addresses this concern by investigating the effects of the boost-phase environment on the thermal conditions of initially densified hydrogen/oxygen ( $H_2/O_2$ ) propellants as a function of the boost-phase flight environment. Both the first and second stages of the rocket are investigated. Since the solution to this problem cannot be obtained easily or inexpensively through ground testing, an analytical study was conducted. The analysis utilized two thermodynamic models that bounded the expected thermodynamic conditions. These models are used to predict minimum and maximum pressurant gas requirements as well as transient liquid temperatures and levels during the boost-phase of flight.

These bounding thermodynamic models were chosen because they are relatively simple and inexpensive to build and execute. They provide general understanding and insight to the problem that a computational fluid dynamics (CFD) model cannot. In some instances, the models developed in this study can predict actual flight conditions. The intention of this study is to use these simple models to obtain significant results, which will help guide the direction of the more detailed and expensive analyses that will eventually be conducted during the implementation of densified propellants.

## Launch Vehicle Data

Keller reports that the most significant conclusion of his research on densified and slush propellants was that "...potential benefits of subcooled hydrogen fuels are highly mission-dependent. Each application must therefore be evaluated individually to determine the extent of these benefits" (ref. 6). Based on this conclusion, it was deemed very important to be able to investigate the effects of the boost-phase flight environment on thermal conditions of densified propellants using environmental heating flight data from an existing launch vehicle. The launch vehicle investigated in this study was the Atlas IIAS.

The Atlas IIAS launch vehicle consists of the Atlas first stage and the Centaur upper stage. The Atlas stage uses oxygen and RP-1 propellants to feed the Rocketdyne MA-5A stage-and-one-half propulsion system. This propulsion system has a two-chamber booster engine and a sustainer engine. The MA-5A engine produces 490,000 lbf of thrust at sea level. The Atlas IIAS also uses four strap-on Castor IVA solid rocket boosters. The Atlas LOX tank is not insulated.

The Centaur upper stage also uses pressure-stabilized tanks to hold the liquid oxygen and liquid hydrogen propellants. The Centaur hydrogen tank is foam insulated while the oxygen tank, for the most part, is not insulated. The Centaur is powered by two RL-10A-4-1 cryogenic  $H_2/O_2$  rocket engines built by Pratt & Whitney. The engines are turbopump fed and provide a total thrust of 44,600 lbf.

## Literature Search

A literature search was conducted as a part of this investigation. The literature search focused on finding works that related the following topics: pressurization and expulsion of cryogenic liquids, densified or slush propellants, aerodynamic heating, and launch or space vehicles. The literature search yielded many works on each of these topics but only a few relating to all or some of the topics. None of the literature reviewed directly addressed the question of what happens to densified propellant thermal conditions during the boost-phase of a vehicle such as the Atlas IIAS. Related reports of interest are summarized below.

Kramer wrote the earliest report that discussed aerodynamic heating of liquid propellants (ref. 7). The report detailed a numerical technique for modeling the aerodynamic heating of a cryogenic propellant tank. The one-dimensional model demonstrated the importance of including the internal or liquid heat transfer coefficient. The model assumed that the heat capacity of the insulation and tank wall could be neglected.

The most interesting work relating to the current investigation was reported by Torre (ref. 8). A space-based orbital transfer vehicle was designed to utilize densified propellants in a cryogenic propellant tankage system constructed with very thin tank walls. The lower operating pressures that resulted from the low vapor-pressure propellants allowed for constructing very thin tank walls that, in turn, lowered the overall vehicle mass. The orbit transfer vehicle was designed to conduct 5 burns in a 72-hr mission.

Torre investigated several pressurization schemes using a code called HYPRS that included ullage/propellant and ullage/wall heat transfer. Torre concluded that for this vehicle a pressurant gas system that utilized all autogenous pressurant gas for both LOX and LH<sub>2</sub> would be required to maximize weight savings. It was also noted in the report that a preliminary analysis indicated that the vapor pressure level of the propellants would change very little during the boost-phase of flight, although no values were reported.

Most of the reports that examined the thermodynamics of densified or slush propellants in launch vehicles were found to be related to that of hypersonic air breathing launch vehicles (refs. 9 to 15). In each of these works a different model was developed or used to study and predict tank thermodynamics. Because of all the different assumptions and techniques used to develop these models, only a top-level review will be given in this report.

Hardy used FLOW-3D, a commercially available, multidimensional, finite-difference fluid flow model to examine the effects of several factors on the temperature profiles in the ullage during ramp pressurization of a liquid hydrogen tank (ref. 9). The research was conducted to demonstrate the capability of the code for use in modeling the propellant thermodynamics of the National Aero-Space Plane. The recommendations made for future modifications to the FLOW-3D code included: liquid/vapor interfacial heat and mass transfer, multi-component ullage, expulsions, and slush hydrogen dynamics, including melting/solidification capability.

Sasmal later improved the FLOW-3D code by incorporating the capability of calculating the heat flux rates from the ullage to the tank wall and to the liquid/slush rather than requiring a priori specification of the boundary heat flux rates (ref. 10). The tank wall was modeled using a lumped heat storage model and the heat fluxes were calculated from standard correlations. The model was used to study the effect of ullage boundary heat flux rates on the pressurization process. Increasing the internal heat flux rates to the wall increased the pressurant mass requirements.

Teare reports on the three-year development of the code TANKQ. TANKQ is a rapid, transient method for conducting a hypersonic vehicle cryogenic tank thermal analysis and is composed of internal and external models (ref. 11). The analysis was developed in order to conduct trade studies for the National Aerospace Plane Program in a timely manner. This was a parallel effort with the FLOW-3D code development effort, which was to be used to benchmark the TANKQ code. The external code modeled the heat transfer into and out of the tank structure and insulation at various phases of the flight profile.

The internal code modeled the ullage and liquid as one node each and used the assumption of thermal equilibrium. The internal code used was called HEATRAN, which was a McDonnell Douglas in-house transient finite difference thermal analyzer. Empirical bulk heating factors were used to ratio the portion of total heat leak that goes into bulk liquid heating. Results of trade studies using TANKQ are also reported. Most notably was the recommendation for a zero net-positive suction head pressure pump since the vapor pressure reached the maximum operating tank pressure by the time the vehicle reached orbit.

Stephens and Hanna developed 1 and 2-D transient thermal models using the code SINDA85/FLUINT to model the Generic Research Cryogenic Tank (GRCT) design (refs. 12 and 13). SINDA/FLUINT, which is now commercially available, is a finite difference thermal analyzer that includes fluid flow and heat transfer. The GRCT was to be used to study the thermal response of a generic liquid hydrogen propellant tank when subjected to simulated hypersonic vehicle heating conditions. The 1-D thermal modeling was used to determine insulation thickness and purge requirements. The 2-D thermal model was used to examine wall temperature gradients, boil-off, and characterization of thermal behavior of the ullage. Out of the 413 nodes, 12 horizontal nodes modeled the ullage and liquid, whereas the remainder modeled the cross-section of the tank wall and insulation. The models did not include liquid expulsion, two-component ullage, or slush hydrogen thermodynamics.

Goodman presents a review of pressurization and uses three existing model formulations from the literature to analyze cryogenic propellant tanks typical of advanced hypersonic vehicles (ref. 14). The three models are: an unvented tank self-pressurization model using the thermal equilibrium assumption, a liquid stratification model, and a tank pressurization/venting model. Each of these will be described.

The self-pressurization model was used to examine self-pressurization during a ground hold. The assumed heat flux was 20 Btu/hr ft<sup>2</sup> for both hydrogen and oxygen tanks. The predicted time for the tank to pressurize from triple point vapor pressure to normal boiling point vapor pressure was 7 hr for hydrogen and 83 hr for oxygen. The total liquid volumes were not given, however, it was stated that the initial fill level was determined such that the final fill level was 100 percent when the triple point liquid expanded to the normal boiling point.

The liquid thermal stratification model utilized boundary layer theory along the walls. The model, when using a heat flux of 20 Btu/hr ft<sup>2</sup> for the given tank size, indicates that complete stratification of the liquid occurred after about 1 hr for both hydrogen and oxygen. Tank venting would then be required after the 1 hr. It is appropriate to mention at this time that Greene has recently modeled liquid stratification for loading densified propellants also using boundary layer theory (ref. 15).

The tank pressurization/venting model is based on a thermodynamic control volume analysis of the ullage and its interaction with the liquid. The model is used to predict the pressurant gas required to maintain constant tank pressure during a simulated transient mission profile of a hypersonic vehicle. The main conclusion was that the assumed transient heat flux (which was not reported) was too high and that more boil-off was generated during the mission than was necessary to maintain tank pressure. It was recommended that a higher fidelity model of the thermal protection system was necessary to provide realistic heat fluxes.

One of the more extensively validated models for predicting pressurant gas requirements is the correlation developed by Epstein and Anderson (ref. 16). This correlation involves dimensionless parameters and a set of empirical constants derived from experimental data. Van Dresar later improved upon the model to account for partially expelled tanks and initially warm tank walls (ref. 17). It was noted in this report that the model was not recommended for use when conditions exist where mass transfer across the liquid/vapor interface is greater than  $\pm 25$  percent of the pressurant mass. It goes on to state that this condition is known to exist for liquid sloshing and slush hydrogen expulsions.

As one can tell from reviewing the literature search, many different models exist for examining tank thermodynamics and pressurant gas requirements. Each model has a different degree of complexity and each has been designed or modified to examine a particular scenario. The modeling approach used in this research was based upon the work of Van Dresar and Haberbush, which bounded the expected pressurant gas consumption for flight weight cryogenic tanks (ref. 18). These models were selected out of the

literature to be the foundation of this research based upon their simplicity, pureness, and their capability to bound the problem.

The two models presented by Van Dresar were an isentropic compression (ideal) model and a thermal equilibrium model. The ideal model predicted the lower bound pressurant gas requirement and the thermal equilibrium model predicted the upper bound pressurant gas requirement. The models advanced the work of Moore (ref. 19) by accommodating a noncondensable pressurant gas and partially filled tanks.

## Symbols

F	fill level fraction
h	enthalpy
m	mass
mr	mass ratio = model prediction/flight data
O/F	oxygen to fuel mass ratio
P	pressure
p	partial pressure
Q	heat leak
S	entropy
TL	temperature of liquid
u	internal energy
V	volume

### Greek

$\rho$	density
--------	---------

### Subscripts

1	state 1
2	state 2
a	vapor or autogenous gas
b	noncondensable gas
g	pressurant gas
H	hydrogen
in	inlet
j	ullage segment
l	liquid
o	outflow
O	oxygen
T	total or tank
u	ullage
v	vent

## Thermodynamic Models

Two thermodynamic models have been developed to be used as tools for bounding the expected thermodynamic conditions of densified propellants during the boost-phase of a launch vehicle trajectory through the atmosphere. These two models are the Isentropic Compression or "Ideal" model and the

Thermal Equilibrium model. Each of these models, as well as the solution techniques and data input files, will now be described.

### Isentropic Compression Model

The isentropic compression model or “Ideal” model, as it will be referred to throughout the report, was originally chosen to predict the minimum or lower bound pressurant gas requirements. However, through the course of this study it was found that under certain conditions this model does not predict the minimum pressurant gas requirements but rather the maximum. This phenomenon will be discussed in more detail later. The ideal model that has been developed in this study is capable of simulating both the pressurization and venting processes with or without liquid expulsion. Previous work (ref. 18) only modeled the pressurization and expulsion process.

**Description.**—The fundamental thermodynamics behind the ideal model are illustrated in figures 3(a) and (b) for the pressurization process going from state 1 to state 2 which in this study represents a one second time interval. The initial state of the liquid is at temperature  $TL_1$  and total tank pressure  $P_1$ . The initial state of the ullage entropy ( $S_1$ ) is also determined from the given tank pressure ( $P_1$ ) and liquid temperature ( $TL_1$ ). The energy from environmental heat leak ( $Q$ ) is absorbed by the liquid and the liquid level and liquid temperature rise. The ullage then undergoes an isentropic (constant entropy) compression to pressure  $P_2$ . The added pressurant gas enters the tank at a specified pressure ( $P_{in}$ ) and temperature ( $T_{in}$ ) to fill the void in the ullage as well as the volume of any expelled liquid until the final tank pressure is met.

Because the transient tank pressure profile in this study is a specified input, the tank must be pressurized or vented at each time step in order to simulate the profile. These transient input data files will be discussed in more detail later. At each time step during the pressurization process, a new ullage segment is generated. At each time step during a vent, mass is subtracted from the most recent ullage segment(s) based on a volume constraint until the tank pressure is met. Because the pressurization and venting process is isentropic, the entropies of the newly formed ullage segments, as well as previously formed ullage segments, must remain constant.

**Equations.**—The pressurant gas mass for a given time step is then calculated from equation (1). Equation (1) is derived from a total ullage volume balance in which the total ullage volume must equal the sum of all ullage volume segments plus the added pressurant gas volume. The ullage masses consist of both vapor and non-condensable components.

$$m_g = \rho_g V_T (1 - F_2) - \rho_g \sum_j \frac{m_{1,j}}{\rho_{2,j}} \quad (1)$$

If the pressurant gas mass is calculated to be a negative number then venting must occur. The mass to be vented is converted to a gas volume based on the density of the gas as calculated from tank pressure and inlet temperature. The vented volume of gas is then subtracted from the existing ullage segment(s) until the appropriate amount of gas has been vented. The ullage segments from which the vent gas is subtracted is of the same type as the pressurant gas, either autogenous or noncondensable, depending on which type is being used at that particular time in the transient launch profile.

**Assumptions.**—The ideal model assumes that mass and energy transfer at the liquid-vapor interface can be neglected. The ullage and added pressurant gas are thermally isolated from their surroundings. Heat exchange between the liquid or ullage gases and the tank wall are also neglected. This assumption is valid for flight weight tanks with thin walls and low heat capacity (ref. 18). The work associated with expansion and contraction of the tank walls (because of their “balloon-like” characteristics) during the pressurization and venting process is also neglected. A conservative analysis of the Centaur stainless

steel flight tank indicated that the amount of work exerted to pressurize the tank to 20 psi was less than 2.5 percent of the environmental heat leak during the boost-phase.

The ideal model assumes that the noncondensable pressurant gas is insoluble in the liquid and that the potential and kinetic energy of the pressurant gas entering the tank is negligible. It is also assumed that autogenous pressurant gas is used during expulsions. The assumption is valid for all vehicles that use rocket engines with autogenous pressurant gas tap-offs. The tap-off provides warm pressurant gas to be supplied to the respective propellant tank for pressurization while the engine is operating and propellants are being expelled from the tanks. Noncondensable pressurant is assumed to be used at all other times.

**Initial conditions.**—The ideal model initial conditions for the transient launch vehicle simulation are as follows. The initial liquid thermodynamic state is determined from the specified initial tank pressure and liquid temperature. The initial ullage is assumed to consist of 100 percent noncondensable gas. The initial ullage state is determined from an assumed uniform temperature equal to that of the liquid and the initially specified tank pressure. This additional assumption of a pure noncondensable ullage is valid based on the inherent ideal model assumption of zero mass and energy transfer across the liquid-vapor interface. This assumption is also valid from a practical perspective. Loading of densified propellants that have vapor pressures below one atmosphere must have a noncondensable gas in the ullage to maintain total tank pressure at or above one atmosphere for structural and safety purposes. At low vapor pressures a large fraction of the ullage will consist of a noncondensable gas.

### Thermal Equilibrium Model

The thermal equilibrium model was originally chosen to predict the maximum or upper bound pressurant gas requirements. In general this is the case, but again, conditions were found in this study under which this model does not predict the maximum pressurant gas requirements but rather the minimum. The thermal equilibrium model developed in this study is capable of simulating both the pressurization and venting processes with or without liquid expulsion.

The thermal equilibrium model improves upon previous work (ref. 18) in a very fundamental way. In this work, the two-component ullage (vapor and noncondensable) is modeled using Dalton's law of partial pressures. The previous work used the Amagat Law, which models the ullage using partial volumes. The current technique is believed to simulate a more realistic scenario in which vapor is allowed to migrate across the liquid-vapor interface with changing liquid temperatures and tank pressures.

**Description.**—The fundamental thermodynamics behind the thermal equilibrium model are illustrated in figures 4(a) and (b) for the pressurization process going from state 1 to state 2 which represents a one second time interval. The initial liquid fill level is at  $F_1$ . The liquid state is determined from total tank pressure ( $P_1$ ) and temperature ( $T_1$ ). The ullage consists of both vapor and noncondensable components also at temperature ( $T_1$ ). The initial state of the vapor component of the ullage is that of saturation at the temperature  $T_1$ . The partial pressure of the vapor in the ullage is the saturation pressure ( $p_{A1}$ ) at temperature  $T_1$ . The partial pressure of the noncondensable ( $p_{B1}$ ) in the ullage is determined by subtracting the vapor partial pressure ( $p_{A1}$ ) from the total tank pressure ( $P_1$ ). The initial state of the noncondensable component of the ullage is then determined from the temperature ( $T_1$ ) and the partial pressure of the noncondensable.

In the pressurization process the tank pressure is increased from  $P_1$  at state 1 to  $P_2$  at state 2. Pressurant gas is added to the tank at pressure ( $P_{in}$ ) and temperature ( $T_{in}$ ). Environmental heat leak ( $Q$ ) also enters the tank. Due to the influx of energy, the liquid level rises to  $F_2$  and the temperature is raised uniformly to  $T_2$ .

**Equations.**—The thermal equilibrium model involves solving a set of linear and non-linear algebraic equations simultaneously. Different sets of equations are solved depending on the process to be modeled. These processes are: (a) a noncondensable pressurant gas ramp, (b) a noncondensable pressurant gas

expulsion, (c) a noncondensable and autogenous vapor vent, (d) an autogenous pressurant gas ramp, and (e) an autogenous pressurant gas expulsion.

Each of these processes involves a number of unknown variables that need to be solved for, using a set of algebraic equations. Table I gives a list of the processes modeled, the unknown variables for a given process, and a list of the equations used to solve for the unknown variables. The equations are now described.

The overall mass balance of the control volume going from state 1 to state 2 is shown in equation (2). The control volume is just inside the propellant tank wall. The left-hand side is the sum of the liquid, vapor, and noncondensable masses at state 1 plus the pressurant gas that enters the tank volume. The pressurant gas is noncondensable for processes A and B, autogenous for processes D and E. The right-hand side is the sum of the liquid, vapor, and noncondensable masses plus the expelled liquid and the vapor and noncondensable vent mass. The vent masses are set to zero for processes A, B, D, and E. The liquid outflow mass is zero for process A, C, and D.

$$m_{l1} + m_{a1} + m_{b1} + m_p = m_{l2} + m_{a2} + m_{b2} + m_o + m_{a_v} + m_{b_v} \quad (2)$$

The next equation is a mass balance of just the noncondensable component. The equation comes in two forms. The first form is equation (3a) which states that the noncondensable ullage mass in state 1 plus any noncondensable pressurant gas added to the tank must equal the noncondensable mass in state 2. Equation (3a) is used in processes A, B, and C. The second form is used when solving process D and E in which autogenous pressurant gas is being used. Equation (3b) states that the initial and final mass of noncondensable remains constant when going from state 1 to state 2.

$$m_{b1} + m_p = m_{b2} \quad (3a)$$

$$m_{b1} = m_{b2} \quad (3b)$$

The next equation is an overall energy balance as derived from the first law of thermodynamics for a control volume and is given in equation (4). The left-hand side of equation (4) gives the liquid, vapor, and non-condensable gas energy at state 1 plus the energy entering the tank from the pressurant gas and the environmental heat leak. The right-hand side is the liquid, vapor, and noncondensable gas energy at state 2 plus the energy of the liquid leaving the control volume. The pressurant gas is noncondensable for processes A and B, autogenous for processes D and E. The vent masses are set to zero for processes A, B, D, and E. The liquid outflow mass is zero for process A, C, and D.

$$m_{l1}u_{l1} + m_{a1}u_{a1} + m_{b1}u_{b1} + m_p h_p + Q = m_{l2}u_{l2} + m_{a2}u_{a2} + m_{b2}u_{b2} + m_o h_o + m_{a_v} h_{a_v} + m_{b_v} h_{b_v} \quad (4)$$

The next equation is an ullage volume constraint. The ullage volume constraint arises from the assumption of using Dalton's model of partial pressures when the ullage consists of both vapor and noncondensable components. Equation (5) states that the final volume of the vapor and the final volume of the noncondensable in state 2 must both equal the total ullage volume. Equation (5) gives the volumes of each component in state 2 in terms of the final mass of the component divided by their respective ullage densities. The densities of the components are determined from their respective partial pressures and temperature at state 2.

$$\frac{m_{a2}}{\rho_{a2}} = \frac{m_{b2}}{\rho_{b2}} = V_u \quad (5)$$

The next equation is a total volume constraint. Equation (6) states that the ullage volume (as represented by the vapor component) plus the liquid volume must equal the total tank volume.

$$\frac{m_{a2}}{\rho_{a2}} + \frac{m_{l2}}{\rho_{l2}} = V \quad (6)$$

The final equation, equation (7), is used in solving process C which is the noncondensable vent. This equation assumes that the amount of vapor and noncondensable mass that is vented is proportional to the ratio of vapor partial pressure to total tank pressure at state 2.

$$\frac{m_{a_v}}{m_{a_v} + m_{b_v}} = \frac{P_{a2}}{P_2} \quad (7)$$

**Assumptions.**—The fundamental assumption of the thermal equilibrium model is that the tank contents (ullage gases and liquid) are at the same temperature. Thus the system of equations inherently contain mass and energy transfer across the liquid-vapor interface. The main assumption made in modeling the venting process is that the amount of vapor and noncondensable mass that is vented is proportional to the ratio of vapor partial pressure to total tank pressure at state 2.

The following assumptions apply to the thermal equilibrium model for the same reasons as stated in the ideal model assumption section. The work associated with expansion and contraction of the tank walls during the pressurization and venting process is neglected. The thermal equilibrium model assumes that the noncondensable pressurant gas is insoluble in the liquid and that the potential and kinetic energy of the pressurant gas entering the tank is negligible. It is also assumed that autogenous pressurant gas is used during expulsions and noncondensable gas is used at all other times.

**Initial Conditions.**—The thermal equilibrium model initial conditions for the transient launch vehicle simulation are as follows. The initial liquid thermodynamic state is determined from the specified initial tank pressure and liquid temperature. The initial ullage is assumed to consist of both vapor and noncondensable gas components. The initial ullage state is determined from an assumed uniform temperature equal to that of the liquid and the partial pressures of each component as detailed in the model description section.

### Flight Profile Input Data

The thermodynamic models described above were written into a computer program using Fortran 90. The program is called PRELUDELV for Pressurized Ramp and Expulsion—Lower and Upper Demarcations for Launch Vehicles. The program was written to accept newly created input files generated from Atlas IIAS flight data. Each of the thermodynamic models was then executed separately such that a change from state one to state two represented a one second interval during the flight.

There were two types of input files; a launch pad hold input file and a launch vehicle profile input file. The first type was used for the launch pad hold analysis. A launch pad hold example input file is given in table II using fabricated input data since the actual data used is proprietary. The launch pad hold input file gives vehicle name, stage description, liquid propellant type, noncondensable pressurant gas type, tank volume, initial ullage volume, initial bulk liquid temperature, heat leak, and tank pressure during hold.

The launch vehicle profile input file was used in the transient thermodynamic analyses. An example of this type of file is shown in table III, again using fabricated input data. The first part of the input file

gives vehicle name, stage description, liquid propellant type, noncondensable pressurant type, tank volume, initial ullage volume, initial bulk liquid temperature, and pressurant inlet pressure. The nominal flight ullage volume was used as the initial ullage volume for all analyses. The pressurant inlet pressure was assumed. It was chosen to be approximately 10 psi higher than the maximum tank pressure seen in the profile. This assumption is based on the fact that pressurant gas inlet enthalpy is a stronger function of temperature than pressure.

The remaining portion of the input files involve the transient input data. The columns of input data are: time in seconds, tank pressure in pounds per square inch absolute, heat leak in Btu/sec, mass outflow rate in pound mass per second, pressurant gas inlet temperature in degrees Rankine, and the pressurant gas type flag (1 for autogenous and 2 for noncondensable). The major constraint of the study was to conduct the thermodynamic analyses using the nominal pressure profiles as required by the Atlas/Centaur vehicle during flight.

## Results

The results of this investigation are presented in the following four sections: Launch Pad Hold, Initial Propellant Temperature Comparisons, Centaur Scenario, and Atlas LOX Tank. The Launch Pad Hold investigation examined the rate of liquid level rise of the densified propellants once the propellant conditioning ground support equipment was terminated prior to launch. The Initial Propellant Temperature Comparison used the bounding thermodynamic models to probe the differences between densified propellants and propellant conditions currently being flown on the Centaur vehicle. Flight data is used to normalize and compare model results. The Centaur Scenario looked at putting densified propellants on the Centaur vehicle at the nominal oxidizer to fuel loading ratios and engine mass flow rates. The final investigation was a comparison between nominal and densified propellant conditions for the Atlas LOX tank during boost.

### Launch Pad Hold

The launch pad hold analysis shows liquid expansion as a function of time after propellant conditioning ground support equipment is terminated prior to lift-off. This investigation was conducted for determining practical hold times once the propellant conditioning equipment has been turned off. This data does not represent in any way a limitation on launch windows due to propellant conditioning ground support equipment.

The thermal equilibrium model was used for this analysis. Both the Centaur liquid hydrogen tank and liquid oxygen tank were investigated. The heat leak for each tank was adjusted slightly from the nominal heat leak to compensate for the colder propellants. The initial bulk liquid hydrogen temperature was 27.0 °R and for oxygen it was 126.0 °R

The tank pressures were held constant which resulted in a constant venting of the tank as the liquid expanded. The current launch pad hold tank pressures for the Centaur vehicle were utilized in order to maintain the structural requirements of the balloon tanks. It is assumed that the ullage initially contains both helium and hydrogen vapor. The vented mass therefore contains both helium and hydrogen vapor in proportion to the partial pressures within the ullage.

Figure 5 shows the liquid level and bulk liquid temperature as a function of time for liquid hydrogen during a launch pad hold after the propellant conditioning equipment has been terminated. The initial fill level is equal to the Centaur nominal fill level. The figure shows the maximum liquid level allowed in flight. This maximum liquid level constraint is in place for pressure control reasons.

The analysis indicates that the hydrogen propellant can sit on the vehicle for a little over 10 min without conditioning. At the 10 min mark, the maximum allowable liquid level at lift-off is reached.

Figure 5 shows that launching at this liquid level will result in reaching the maximum flight liquid level for the vehicle at the end of the boost-phase. The Centaur then fires after the boost-phase and liquid levels begin decreasing due to propellant expulsion. The liquid hydrogen temperature rose 2.4 °R from 27 to 29.4 °R during the 10 min.

Figure 6 shows the Centaur liquid oxygen tank during a launch pad hold simulation with densified oxygen. This analysis indicates that oxygen conditioning can be terminated nearly 40 min prior to lift-off and still maintain acceptable liquid levels for flight. The liquid temperature raised 3.5 °R from 126 to 129.5 °R during the 40 min.

### Initial Propellant Temperature Comparisons

The thermodynamic models were used to examine the differences in liquid level, bulk liquid temperature, and pressurant gas consumption as a function of the initial bulk liquid propellant temperature for the Centaur liquid hydrogen and liquid oxygen tanks during the boost-phase and first burn. Centaur flight data is used to normalize and compare the model results. In this analysis, the liquid expulsion rates for both the nominal and densified propellants are identical.

The initial bulk liquid temperature was the main parameter to be varied in this analysis. The nominal Centaur hydrogen propellant temperature was compared to a densified hydrogen propellant temperature of 27.0 °R. The nominal Centaur oxygen propellant temperature was compared to a densified oxygen propellant temperature of 126.0 °R. The heat leak into the propellants were adjusted slightly for the colder propellants. The initial ullage volumes for both nominal and densified propellants were the same. The initial ullage volumes used were the nominal Centaur ullage levels.

**Liquid level.**—The first results to be discussed are the predicted changes in liquid level as a function of initial bulk liquid temperature for the Centaur hydrogen and oxygen tanks during the boost-phase. These results are presented in tabular form in table IV as the maximum delta liquid level change from the initial fill level. The results are given for both the ideal model and the thermal equilibrium model.

Examining hydrogen first, the ideal model predicts approximately the same rise in liquid level due to environmental heat leak for both nominal and densified hydrogen. The liquid level rise for the densified propellant is slightly less due to the increased liquid thermal mass available for absorbing the heat leak.

The thermal equilibrium model predicts a larger delta rise in fill level (0.8 percent) for the densified propellant than for the nominal propellant (0.2 percent). The thermal equilibrium model includes liquid heating from environmental heat leak as well as pressurant gas energy. In the nominal propellant case, less pressurant gas is required to maintain the pressure profile and thus less energy is imparted to the liquid, which causes the liquid level to rise. In the densified propellant case, more pressurant gas is required and thus more energy is added to the liquid causing the liquid level to rise more than in the colder case. More importantly, the maximum predicted delta fill level increase of 0.8 percent is sufficiently under the maximum allowable fill level delta in the Centaur tank.

The oxygen results are fairly straightforward. The rise in liquid level for both nominal and densified propellants and for both ideal and thermal equilibrium models is less than 0.1 percent. The predicted liquid level rise for oxygen is also below the maximum allowable fill level delta for the Centaur oxygen tank.

**Liquid temperature.**—Liquid temperature predictions at the end of boost-phase and first burn are presented in table V as a function of nominal and densified propellants for both hydrogen and oxygen. Also shown is the delta temperature change between the beginning and ending of each particular phase. The flight data liquid temperature is measured from sensors inside the propellant tank sump regions.

The liquid temperature rise for both nominal and densified hydrogen during the boost-phase, independent of model type, remains at or below 1.0°. This indicates that the densified propellant will essentially remain in its subcooled state during the boost. The ideal model in general predicts the flight data

better than the thermal equilibrium model. This is primarily due to a well-designed ullage pressurization system used in the Centaur hydrogen tank that minimizes heat transfer at the liquid-vapor interface.

The liquid temperature rise of hydrogen during the first burn is greatly over predicted by the thermal equilibrium model and is unrealistic. This again is due to the inherent assumptions of the model, which include complete heat and mass transfer between the autogenous pressurant gas and the liquid thus causing increased liquid heating. The ideal model predicts the first burn flight data rather well indicating almost no difference in liquid temperature during the first burn between the nominal and densified propellant cases.

The Centaur oxygen system is submerged pressurization with noncondensable helium. During the boost-phase the models are predicting between  $\pm 0.2^\circ$  for both nominal and densified cases. This indicates that there are insignificant differences in liquid temperature rise between nominal and densified propellants. The flight data shows an increase of  $0.8^\circ$ . This increase is believed to be larger than that experienced by the bulk liquid because the measurement was made inside the sump, located within the thrust barrel, which tends to restrict mixing with the bulk liquid.

The liquid temperature flight data during the first burn indicates a  $1.5^\circ$  decrease in temperature. The thermal equilibrium model predicts a  $1.7^\circ$  decrease. This data, as well as the pressurant gas data to be presented next, indicates that the thermal equilibrium model represents the submerged pressurant gas technique quite well. In the case of the densified oxygen the thermal equilibrium model shows a  $1.2^\circ$  increase. Even so, the densified oxygen in general remains in its subcooled state during the first burn.

**Pressurant gas.**—Table VI gives the pressurant gas consumption predictions for Centaur hydrogen and oxygen tanks. The table compares autogenous and noncondensable pressurant gas consumption for both nominal and densified propellants. The data is presented in normalized form. The pressurant gas consumption flight data is used to normalize the model data. The normalization provides a method for referencing the predicted data to the flight data.

In the case of hydrogen in which ullage pressurization takes place, the ideal model predicts a minimum and the thermal equilibrium model predicts a maximum. In the case of oxygen in which submerged pressurization takes place, the ideal model actually predicts a maximum and the thermal equilibrium model predicts the minimum. These phenomena will be discussed later.

In the case of hydrogen, the non-condensable pressurant gas flight data during the boost-phase is interpolated to be 11.7 percent of the difference between the thermal equilibrium and ideal bounding model predictions. The noncondensable pressurant gas during the first burn is interpolated to be 10.4 percent of the difference between the bounding models. The autogenous pressurant gas flight data is 20.3 percent of the difference between the bounding model predictions. These percentages will be referred to as scaling factors later in the report. The autogenous pressurant gas consumption during the first burn predicted by the thermal equilibrium model is over-predicted and unrealistic since ullage pressurization is the actual method. However, it does provide the upper bound and will be used in creating scaling factors for engineering approximations.

The Centaur oxygen pressurant gas consumption predictions during first burn are most interesting. The thermal equilibrium model actually predicts the minimum consumption at the nominal propellant temperature (high vapor pressure). The model predicts within 6 percent of the actual flight data. The thermal equilibrium model represents the Centaur submerged pressurization process, where one would expect excellent heat transfer between the helium bubbles and the LOX. Interestingly enough, the thermal equilibrium model predicts the maximum pressurant gas consumption at the lower propellant liquid temperature. This phenomenon is due to the thermal equilibrium model ullage volume constraint.

The thermal equilibrium model ullage volume constraint as given in equation (8) says that the oxygen vapor and noncondensable helium gas must occupy the same ullage volume. Equation (8) can also be written in the form given in equation (9) which is also the same as equation (5).

$$V_a = V_b = V_u \quad (8)$$

$$\frac{m_a}{\rho_a} = \frac{m_b}{\rho_b} = V_u \quad (9)$$

When the liquid temperature is warm, the ullage vapor partial pressure is relatively large compared to the noncondensable partial pressure. This means that given the same temperature, the oxygen vapor density is relatively large compared to the helium density. In order for equation (9) to balance, large amounts of oxygen vapor must be generated for a given amount of injected helium pressurant gas. In the nominal Centaur oxygen propellant case nearly 98 percent of the pressurant is generated from vaporizing liquid oxygen and 2 percent is from helium pressurant gas. This is illustrated in figure 7 especially during the first burn.

When the liquid temperature is colder, the LOX vapor pressure decreases. To maintain tank pressure, the noncondensable partial pressure becomes relatively large compared to the oxygen vapor partial pressure. This results in a relative increase in helium density and decrease in oxygen vapor density. Thus, for a given injected amount of helium, less oxygen vapor is generated. In the Centaur oxygen propellant cold case, the vaporized liquid oxygen is 22 percent of the total pressurant and the helium pressurant gas makes up 78 percent. This is illustrated in figure 8.

### **Centaur Scenario**

The objective of this analysis is to examine the Centaur vehicle in a realistic boost-phase scenario involving densified hydrogen and oxygen propellants. The basic assumption of this analysis is that densified propellants are loaded into the existing Centaur propellant tanks in such a manner as to minimize operational impact (i.e. maintain nominal O/F and engine flow rates). As in the previous analysis, this analysis will look at the transient behavior of liquid level, liquid temperature, and pressurant gas consumption during the boost-phase and first burn. The liquid oxygen pressurization will be modeled using the thermal equilibrium model. The liquid hydrogen pressurization will use the scaling factors as described in section 3.2 to interpolate between the two models for estimating pressurant gas consumption.

### **Propellant Loading**

In the densified Centaur scenario the hydrogen tank is loaded with densified hydrogen at 27.0 °R. This temperature represents a realistic average loading temperature for densified hydrogen. Using the nominal Centaur propellant-loading ratio, the liquid oxygen can then be densified to 136.3 °R. Loading the Centaur with densified oxygen and hydrogen at these temperatures and at the nominal Centaur tank pressures resulted in increasing the propellant mass by 8.9 percent. A "rule-of-thumb" estimate indicates that an increase in propellant mass of this magnitude would result in a payload increase of approximately 330 lbm (ref. 20).

### **O/F Loading Sensitivity**

In the course of the previous analysis it was discovered that the final loaded liquid oxygen temperature is very sensitive to the required loading O/F. Figure 9 is a plot of the liquid oxygen temperature as a function of the oxidizer to fuel loading ratio at the nominal LOX fill level and the maximum allowable fill level. This plot is for a fixed densified hydrogen loaded mass at 27 °R. The plot indicates that for just a 0.02 change in the O/F ratio, the required LOX temperature changes 2°R.

The horizontal line in figure 9 is the theoretical minimum temperature of the LOX that can be achieved using a LN<sub>2</sub> normal boiling point bath oxygen subcooler, which represents the simplest technique for densifying oxygen. Due to environmental heat leak into the tanks and fill lines the actual oxygen temperature will be slightly higher than the theoretical minimum. The densified propellant-loading ratio for the Centaur using 27 °R hydrogen requires a densified LOX temperature of 136.3 °R. In this scenario a LOX subcooling technique that goes below the minimum temperature obtainable with a LN<sub>2</sub> normal boiling point bath will be required to condition the propellants.

The trade-off in this scenario is between vehicle performance increases and oxygen densification technique simplicity. To maximize vehicle performance increases attributed to the increased density of the propellants, the hydrogen must be densified as far as possible and then the oxygen must be densified to the appropriate oxygen-to-fuel propellant-loading ratio. The current scenario results in using an oxygen propellant conditioning system that can obtain temperatures below the normal boiling point of liquid nitrogen. On the other hand, simplifying the oxygen conditioning system can be accomplished through the use of the LN<sub>2</sub> normal boiling point bath. However, in order to maintain the nominal loading O/F ratio the hydrogen cannot be densified to the maximum extent, thus decreasing vehicle performance gains from the maximum possible.

### Flight Profile Thermal Model Results

The nominal tank pressure profiles for both oxygen and hydrogen were maintained for the nominal mission length through the first burn. The transient profile engine firings were then extended an additional amount of time at constant levels to consume the additional propellant that was loaded as a result of the propellant densification. The nominal propellant flow rates of the two RL10A-4 engines on the Centaur were maintained.

The results of the analysis are summarized in table VII. The pressurant gas consumption data is normalized by the nominal Centaur flight data for both boost-phase and first burn separately. The thermal equilibrium model predicts the noncondensable helium pressurant gas requirement using submerged pressurization into the densified liquid oxygen during the boost-phase to be 4.4 times the current amount used on the Centaur and 7.6 times the current amount used during the first burn. The ideal model predicts only 0.6 times for boost-phase and 2.6 times the current amount for first burn. The LOX temperature rise as predicted by the thermal equilibrium model in this case is 0.3 °R during the boost-phase and 1.0 °R during first burn.

The thermal equilibrium model for noncondensable helium pressurization of the hydrogen ullage during boost predicts 7.5 times the nominal amount used on the Centaur during the boost-phase and for first burn ramp pressurization. The ideal model predicts 0.5 and 0.1 times the nominal amount of helium for boost-phase and first burn, respectively. The scaling factors (generated in section 3.2) of 0.117 during boost-phase and 0.104 during first burn were used to estimate the actual helium consumption ratios in the densified Centaur scenario, according to equation (10). The estimated helium consumption during boost was 1.3 times the nominal Centaur helium consumption during boost-phase and 1.2 times the nominal amount during first burn.

$$mr = (\text{scalingfactor}) * (mr^{TE} - mr^{Ideal}) + mr^{Ideal} \quad (10)$$

In the case of autogenous hydrogen ullage pressurization during first burn, the scaling factor is 0.203. The thermal equilibrium model predicted 6.6 times nominal pressurant required and the ideal model predicted 0.7 times the nominal required. Using equation (10) the estimated autogenous pressurant gas consumption is 1.9 times the nominal amount currently used on Centaur. The RL10 engines on the Centaur must be able to provide this additional hydrogen pressurant. Further investigation into the RL10 engine

capabilities for handling vehicle requirements for densified propellants such as the previously stated pressurization flow rates are clearly required and are out of the scope of this study.

### Atlas LOX Tank

The Atlas first stage liquid oxygen tank was also investigated using the bounding thermodynamic models. Transient input files for densified oxygen and the current flight configuration were executed. The analysis assumed equal expulsion flow rates for both cases. The analysis is not an "Atlas Scenario" that adjusts the liquid oxygen tank volume for the densified propellant such that the nominal oxidizer-to-fuel loading ratio is constant. It is just a comparison between densified oxygen and the nominal liquid oxygen conditions currently used in flight.

The results of the analysis are shown in table VIII. The pressurant gas consumption is normalized using the flight data. The liquid temperature rise is given in terms of the delta change from the initial propellant temperature. The ideal and thermal equilibrium model pressurant gas consumption results for the nominal propellant case bound the flight data. The thermal equilibrium model predicts 20 percent more pressurant gas than the ideal for the nominal propellant and over 290 percent for the densified propellant.

The thermal equilibrium model predicts a smaller rise in liquid temperature over that of the ideal model for the nominal propellant. This is due to the evaporative cooling effect caused by the vaporization of the liquid to make up pressurant gas. The ideal model predicts the same liquid temperature rise for both the nominal and densified propellants. The maximum liquid temperature rise is 5.0 °R as predicted by the thermal equilibrium model for the densified propellant.

### Conclusions

Modified thermodynamic models were developed to bound the expected thermodynamic conditions of launch vehicle cryogenic propellant tanks during the initial phases of flight. The models were modified to simulate ramp pressurization, liquid expulsion, and tank venting. The ideal isentropic compression model was developed to predict minimum pressurant gas requirements. The thermal equilibrium model was developed to predict the maximum pressurant gas requirements. A thermal equilibrium model modification, which involved modeling a two-component ullage using partial pressures, led to the discovery of a situation in which the thermal equilibrium model predicts the minimum pressurant gas requirement and the ideal model predicts the maximum pressurant gas requirement.

The thermodynamic models were used to examine the bounding thermodynamic conditions of both densified propellants and the nominal propellants loaded into the Atlas IIAS first stage liquid oxygen tank and Centaur upper stage liquid oxygen and liquid hydrogen tanks. The parameters examined during Atlas boost and Centaur first engine burn phases were liquid temperature, liquid level, and pressurant gas. The models were also used to conduct a densified propellant Centaur scenario in which densified hydrogen and oxygen were loaded onto the Centaur at the nominal O/F loading ratio. The following conclusions are made with respect to the densified-to-nominal-propellant comparisons.

**1. There is no significant difference in the liquid level increases during the boost-phase of flight between densified and nominal propellants.**

This is true independent of the thermodynamic model type and it is also true for both hydrogen and oxygen propellants. The data shows that the liquid fill level in both the oxygen and hydrogen cases will not expand during the boost-phase above the maximum allowable fill level. Densified propellants are feasible to fly, based on expected changes in liquid level during the boost-phase.

**2. Propellant temperature change during boost-phase indicates that there is not a significant difference between densified and nominal propellants.**

Liquid oxygen temperature change results indicate no significant difference between densified and nominal propellants. Liquid hydrogen temperature changes during boost-phase, indicates a slightly higher increase for the densified propellant but the magnitude of change is an acceptable one degree. Liquid oxygen and liquid hydrogen temperature changes during the first burn of the Centaur are also insignificant assuming the ideal model is valid for simulating liquid heating (i.e., pressurant gas heat transfer to the liquid is negligible). The flight data does seem to validate the use of the ideal model for liquid temperature change. Thus, for both the boost-phase and Centaur first burn, liquid temperature rise does not appear to be a significant obstacle for densified propellants.

**3. In terms of tank fluid thermodynamics, it appears that pressurant gas requirements are the critical factor in determining the feasibility of flying with densified propellants.**

The Centaur Scenario will be used to discuss pressurant gas requirements. The thermal equilibrium model was found to accurately predict pressurant gas consumption for submerged pressurization of liquid oxygen with gaseous helium. The thermal equilibrium model, when used to predict helium pressurant gas requirements for densified liquid oxygen on the Centaur, resulted in the use of an inordinate amount of gaseous helium. This leads to the following conclusion.

**4. Submerged pressurization of densified oxygen is highly undesirable and should be avoided.**

Densified liquid hydrogen pressurant gas consumption, as predicted using the bounding pressurant gas models and scaled with flight data, indicate that, in general, increases in pressurant gas consumption will be required for densified liquid hydrogen if the nominal tank pressure profiles must be maintained. The increase in helium requirements over the nominal amount are estimated to be in the 30 percent range while autogenous pressurant gas requirements could be in the 300 percent range. Therefore, the following conclusion is made.

**5. Methods for minimizing pressurant gas consumption should be explored.**

One such method is to allow the tank pressure to naturally decay as liquid is being expelled during the first burn. This option is feasible due to net positive suction pressure (NPSP) available from the sub-cooled liquid temperatures (i.e., liquid subcooling does not have to come from increasing tank pressures).

Analyses that were conducted involving the loading of densified propellants led to the following conclusions. The launch pad hold analysis demonstrated the feasibility of terminating the densified propellant conditioning ground support equipment prior to lift-off. The densified hydrogen propellant temperature and liquid level stay under the maximum limits for approximately 10 min after GSE termination. The densified oxygen stays under the maximum limits for nearly 40 min. It was also determined that the required temperature of the densified oxygen is very sensitive to selection of the propellant O/F loading ratio. This leads to the conclusion that O/F loading ratio is a strong driver in determining the liquid oxygen propellant densification equipment selection.

## **Recommendations**

Research has been conducted in which fundamental thermodynamic principals have been applied to a very practical problem, that of bounding the expected thermodynamic conditions of densified propellants during the boost-phase of flight. The research has lead to many insightful conclusions, techniques for bounding thermodynamic conditions that can be used in many other applications, and finally, some recommendations.

It is recommended that techniques for minimizing pressurant gas consumption for densified propellants be examined. In particular, one scenario to be investigated is that of allowing the Centaur oxygen

and hydrogen tank pressures to decay during the first burn instead of maintaining the nominal pressure levels. It is also recommended that the Centaur liquid oxygen tank switch from submerged pressurization to ullage pressurization when flying densified propellants.

In terms of modeling, it is recommended that an uncertainty analysis be conducted on the thermodynamic model results. A sensitivity analysis should also be conducted based on the range of possible input values. For example, the liquid temperature change during the boost-phase can be determined over the range of possible environmental heat leak rates. Additional validation of the models using existing test data should also be accomplished as time permits. Any new and existing pressurization data involving densified propellants should be collected and compiled into a single database for future reference.

## References

1. McNelis, N., Habermusch M., "Hot Fire Ignition Test with Densified Liquid Hydrogen Using a RL10B-2 Cryogenic H<sub>2</sub>/O<sub>2</sub> Rocket Engine," NASA TM 107470, AIAA-97-2688, July 1997.
2. Friedlander, A., Zubrin, R., Hardy, T., "Benefits of Slush Hydrogen for Space Missions," NASA TM-104503, October 1991.
3. Fazah, M., "STS Propellant Densification Feasibility Study Data Book," NASA TM-108467, September 1994.
4. DeWitt, R., Hardy, T., Whalen, M., Richter, P., "Slush Hydrogen (SLH<sub>2</sub>) Technology Development for Application to the National Aerospace Plane (NASP)," NASA TM-102315, July 1989.
5. Huzel, D., Huang, D., "Design of Liquid Propellant Rocket Engines," NASA SP-125, 1971.
6. Keller, C., "Effects of Using Subcooled Liquid and Slush Hydrogen Fuels on Space Vehicle Design and Performance," AIAA-67-467, July 1967.
7. Kramer, J., Lowell, H., Roudebush, W., "Numerical Computation of Aerodynamic Heating of Liquid Propellants," NASA TN D-273, January 1960.
8. Torre, C., Witham, J., Dennison, E., McCool, R., Rinker, M., "Analysis of a Low-Vapor-Pressure Cryogenic Propellant Tankage System," Journal of Spacecraft, Vol. 26, No. 5, 1989.
9. Hardy T., Tomsik, T., "Prediction of the Ullage Gas Thermal Stratification in a NASP Vehicle Propellant Tank Experimental Simulation Using FLOW-3D," NASA TM-103217, July 1990.
10. Sasmal, G., Hochstein, J., Hardy, T., "Influence of Heat Transfer Rates on Pressurization of Liquid/Slush Hydrogen Propellant Tanks," AIAA-93-0278, January 1993.
11. Teare D., Kubik, D., "Integrated Cryo-Tank Thermodynamic Analysis Method," AIAA-90-5215, October 1990.
12. Stephens, C., Hanna, G., "Thermal Modeling and Analysis of a Cryogenic Tank Design Exposed to Extreme Heating Profiles," AIAA-91-1383, July 1991.
13. Hanna, G., Stephens, C., "Predicted Thermal Response of a Cryogenic Fuel Tank Exposed to Simulated Aerodynamic Heating Profiles with Different Cryogenes and Fill Levels," NASA CR-4395, September 1991.
14. Goodman, J., Hashemi, A., "Pressurization Characteristics of Cryogenic Propellant Tanks for an Advanced Hypersonic Vehicle," 28th National Heat Transfer Conference, ASME Heat Transfer Division, Vol. 207, pp. 137-146, 1992.
15. Greene, W., Knowles, T., Tomsik, T., "Propellant Densification for Launch Vehicles: Simulation and Testing 1999," AIAA-95-2335, June 1999.
16. Epstein, M., Anderson, R., "An Equation for the Prediction of Cryogenic Pressurant Requirements for Axisymmetric Propellant Tanks," Advances in Cryogenic Engineering, Vol. 13, 1968.
17. Van Dresar, N., "Prediction of Pressurant Mass Requirements for Axisymmetric Liquid Hydrogen Tanks," Journal of Propulsion and Power, Vol. 13, No. 6, 1997.

18. Van Dresar, N., Habermusch, M., "Thermodynamic Models for Bounding Pressurant Mass Requirements of Cryogenic Tanks," NASA TM-106476, July 1993.
19. Moore, R., et al., "Gas-Pressurized Transfer of Liquid Hydrogen," Advances in Cryogenic Engineering, Vol. 5, 1960.
20. Conversation with Lockheed Martin engineers.

TABLE I.—THERMAL EQUILIBRIUM MODEL PROCESSES.  
X = UNKNOWN VARIABLE FOR GIVEN PROCESS

	Process	Liquid mass	Vapor mass	Noncon mass	Pressure gas mass	Vapor vent mass	Noncon vent mass	Final temperature	Equations
		$m_{l,2}$	$m_{a,2}$	$m_{b,2}$	$m_p$	$m_{a,v}$	$m_{b,v}$	$T_2$	
A	Noncon ramp	x	x	x	x			x	2,3a,4,5,6
B	Noncon expulsion	x	x	x	x			x	2,3a,4,5,6
C	Noncon vent	x	x	x		x	x	x	2,4,3a,5,6,7
D	Autogenous ramp	x	x		x			x	2,3b,4,5,6
E	Autogenous expulsion	x	x		x			x	2,3b,4,5,6

TABLE II.—LAUNCH PAD HOLD EXAMPLE INPUT FILE

C LAUNCH PAD HOLD		
C EXAMPLE FILE		
C		
VEHICLE NAME		WOLF ONE
STAGE DESCRIPTION		SECOND
LIQUID PROPELLANT		PH2
NON-CONDENSABLE PRESSURANT		HE
TANK VOLUME	[FT3]	600.0
INITIAL ULLAGE VOLUME	[FT3]	6.0
INITIAL BULK LIQUID TEMP	[R]	27.0
HEAT LEAK	BTU/SEC]	5.0
TANK PRESSURE DURING HOLD	[PSIA]	18.0

TABLE III.— LAUNCH VEHICLE INPUT FILE EXAMPLE FILE		
C LAUNCH VEHICLE INPUT FILE		
C EXAMPLE FILE		
C		
VEHICLE NAME		WOLF ONE
STAGE DESCRIPTION		SECOND
LIQUID PROPELLANT		H2
NON-CONDENSABLE PRESSURANT		HE
TANK VOLUME	[FT3]	600.0
INITIAL ULLAGE VOLUME	[FT3]	6.0
INITIAL BULK LIQUID TEMP	[R]	27.0
PRESSURANT INLET PRESSURE	[PSIA]	40.0
TRANSIENT DATA FROM T=0 LIFT-OFF. TIME MUST BE INTEGER		

TOTAL TRANSIENT DATA POINTS 18					
TIME [SEC]	TANK PRESSURE [PSIA]	HEAT LEAK [BTU/SEC]	MASS OUTFLOW [LBM/SEC]	GAS TEMPERATURE [R]	PRESSURANT GAS TYPE, 1=AUTO, 2=NC
0.00	18.00	5.0	0000.0	520.0	2.0
10.00	19.00	6.0	0000.0	540.0	2.0
20.00	20.00	7.0	0000.0	560.0	2.0
30.00	21.00	8.0	0000.0	580.0	2.0
40.00	22.00	9.0	0000.0	600.0	2.0
50.00	23.00	10.0	0000.0	620.0	2.0
60.00	24.00	9.0	0000.0	620.0	2.0
70.00	25.00	8.0	0000.0	620.0	2.0
80.00	25.00	7.0	0000.0	600.0	2.0
90.00	25.00	6.0	0000.0	580.0	2.0
100.00	25.00	5.0	0000.0	560.0	2.0
110.00	24.00	4.0	0000.0	540.0	2.0
120.00	23.00	3.0	0000.0	520.0	2.0
130.00	22.00	3.0	0000.0	520.0	2.0
140.00	21.00	3.0	0000.0	520.0	2.0
150.00	20.00	3.0	3.0	520.0	1.0
200.00	20.00	3.0	3.0	520.0	1.0
250.00	20.00	3.0	3.0	520.0	1.0

TABLE IV.—LIQUID LEVEL CHANGES AS A FUNCTION OF INITIAL BULK LIQUID TEMPERATURE CENTAUR HYDROGEN AND OXYGEN TANKS DURING BOOST-PHASE

Initial bulk liquid temperature	Maximum delta liquid level changes during boost-phase	
	Ideal model (percent)	Thermal equilibrium model (percent)
<b>HYDROGEN</b>		
Nominal	0.6	0.2
27.0 °R	0.5	0.8
<b>OXYGEN</b>		
Nominal	< 0.1	< 0.1
126.0 °R	< 0.1	< 0.1

TABLE V.—LIQUID TEMPERATURE CHANGE AS A FUNCTION OF INITIAL LIQUID TEMPERATURE CENTAUR HYDROGEN AND OXYGEN TANKS AT END OF BOOST-PHASE AND FIRST BURN

Initial liquid temperature	Liquid temperature at end of boost-phase			Liquid temperature at end of first burn		
	Ideal model	Flight data	Equilibrium model	Ideal model	Flight data	Equilibrium model
<b>HYDROGEN</b>	$\Delta T$	$\Delta T$	$\Delta T$	$\Delta T$	$\Delta T$	$\Delta T$
Nominal	0.5°	0.8°	0.2°	-0.1°	0.0°	2.7°
27.0°R	0.7°		1.0°	0.0°		12.5°
<b>OXYGEN</b>						
Nominal	-0.2°	0.8°	0.2°	-0.2°	-1.5°	-1.7°
126.0°R	0.2°		0.2°	-0.1°		1.2°

TABLE VI.—PRESSURANT GAS CONSUMPTION AS A FUNCTION OF INITIAL LIQUID TEMPERATURE CENTAUR HYDROGEN AND OXYGEN TANKS AT END OF BOOST-PHASE AND FIRST BURN NORMALIZED TO NOMINAL CASE FLIGHT DATA

Initial liquid temperature	Pressurant gas consumption at end of boost-phase						Pressurant gas consumption at end of first burn					
	Ideal model		Flight data		Equilibrium model		Ideal model		Flight data		Equilibrium model	
<b>HYDROGEN</b>	Auto	Non	Auto	Non	Auto	Non	Auto	Non	Auto	Non	Auto	Non
Nominal		0.36		1.0		5.82	0.70	0.38	1.0	1.0	2.18	6.38
27.0°R		0.36				7.45	0.64	0.38			6.49	17.75
<b>OXYGEN</b>												
Nominal		0.56		1.0		2.22		2.65		1.0		0.94
126.0°R		0.56				2.78		2.35				7.85

TABLE VII.—DENSIFIED PROPELLANT CENTAUR  
SCENARIO RESULTS SUMMARY RELATIVE TO  
NOMINAL CENTAUR OPERATIONS

	Boost-phase	First burn
Oxygen		
Helium pressurant gas ratio		
Thermal equilibrium	4.4	7.6
Ideal model	0.6	2.6
Liquid temperature T.E. Model (R)	136.6	137.6
Hydrogen		
Helium pressurant gas ratio		
Thermal equilibrium	7.5	7.5
Ideal model	0.5	0.1
Scaling factor prediction	1.3	0.87
Hydrogen pressurant gas ratio		
Thermal equilibrium		6.6
Ideal model		0.7
Scaling factor prediction		1.9

TABLE VIII.—ATLAS OXYGEN TANK RESULTS SUMMARY  
PRESSURANT GAS NORMALIZED TO FLIGHT DATA

	Ideal model	Flight data	Thermal equilibrium model
Helium pressurant gas ratio			
Nominal	0.85	1.0	1.02
126.0 °R	0.77		3.01
Final liquid temperature ( $\Delta$ °R)			
Nominal	2.9	(a)	1.6
126.0 °R	2.8		5.0

<sup>a</sup>Unavailable.

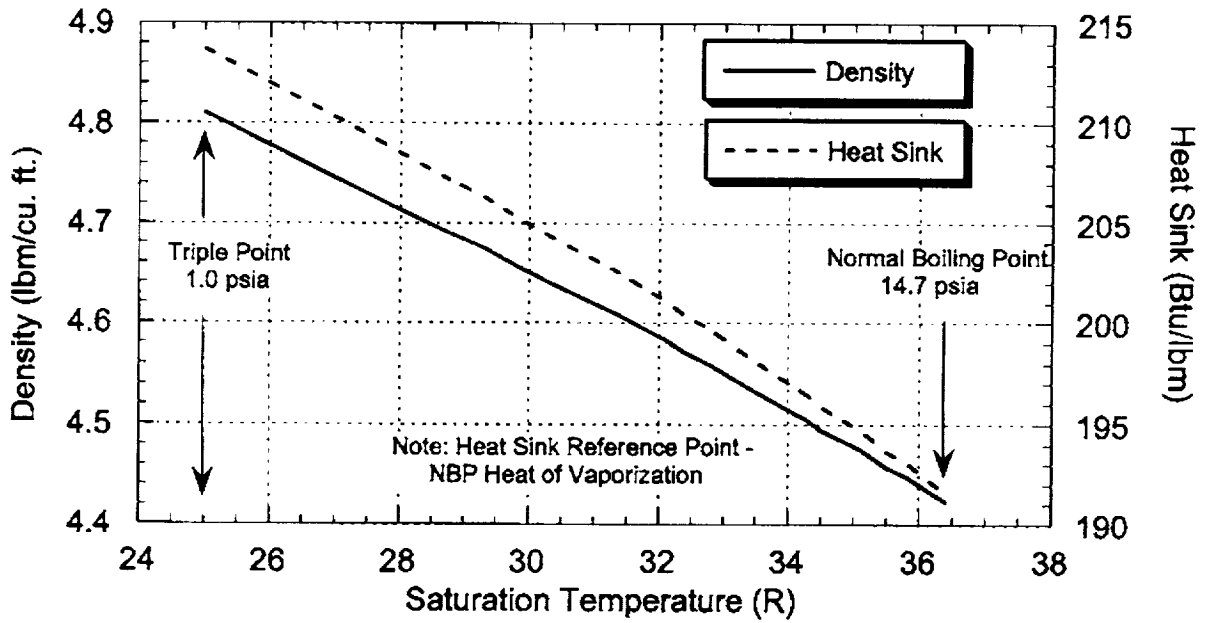


Figure 1.—Densified liquid hydrogen properties.

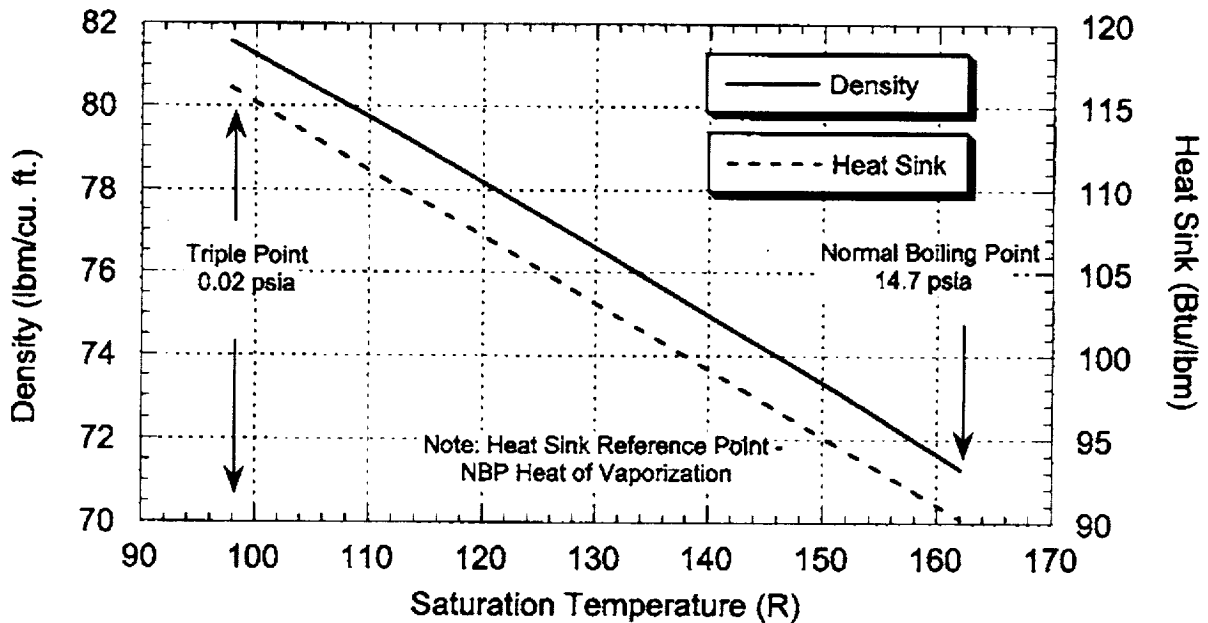


Figure 2.—Densified liquid oxygen properties.

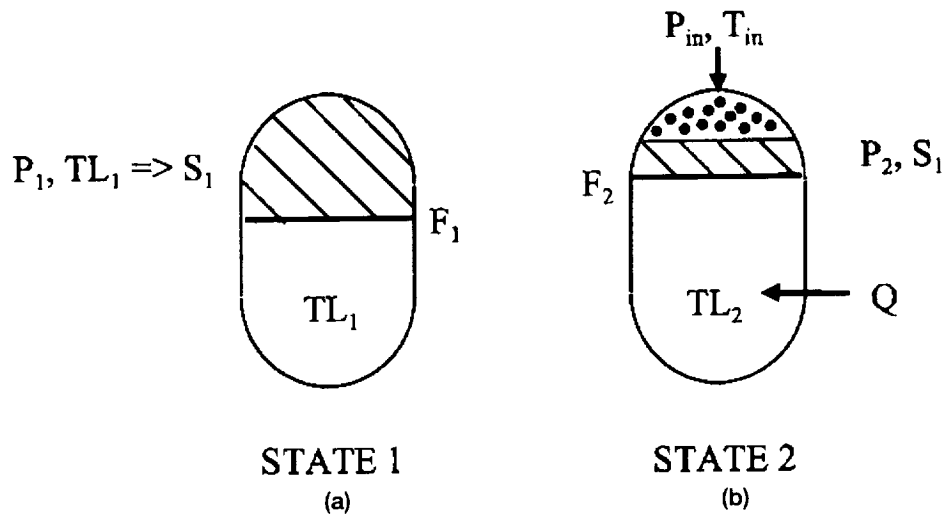


Figure 3.—Isentropic compression "ideal" model - tank pressurization.

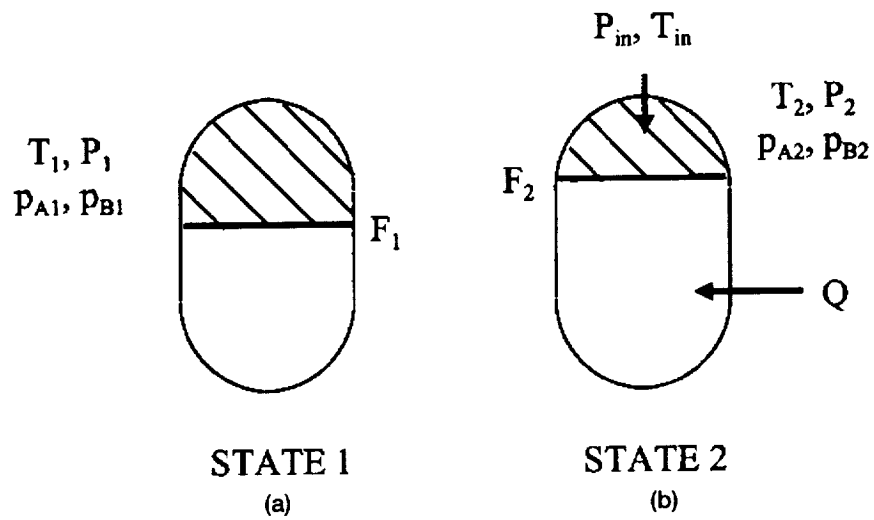


Figure 4.—Thermal equilibrium model - tank pressurization.

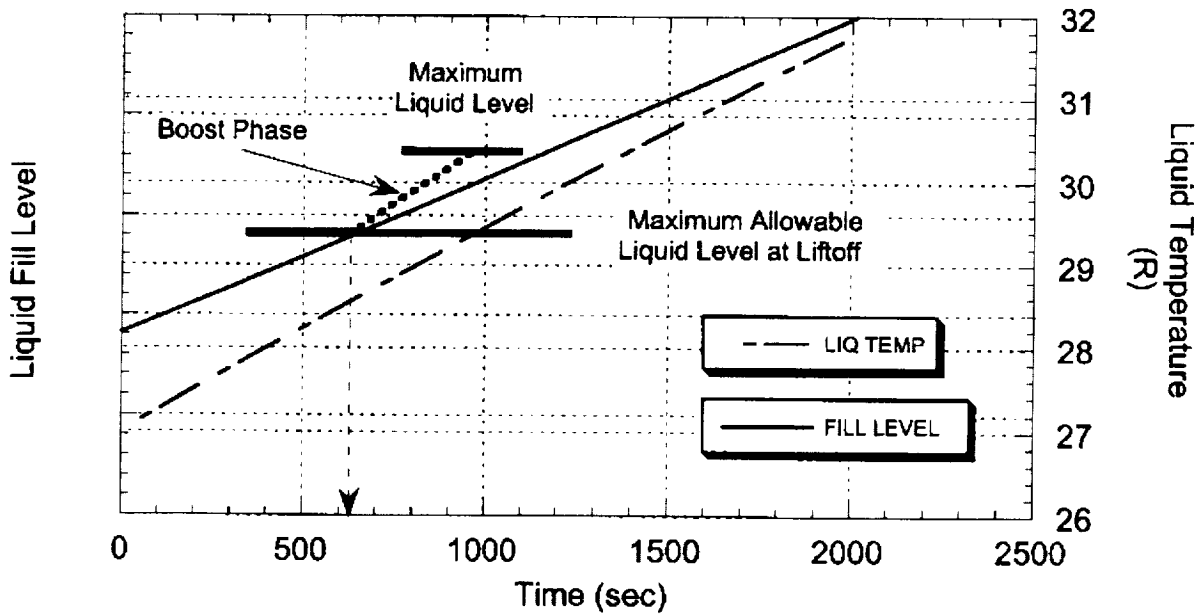


Figure 5.—Launch pad hold Centaur hydrogen tank - densified hydrogen at 27 R.

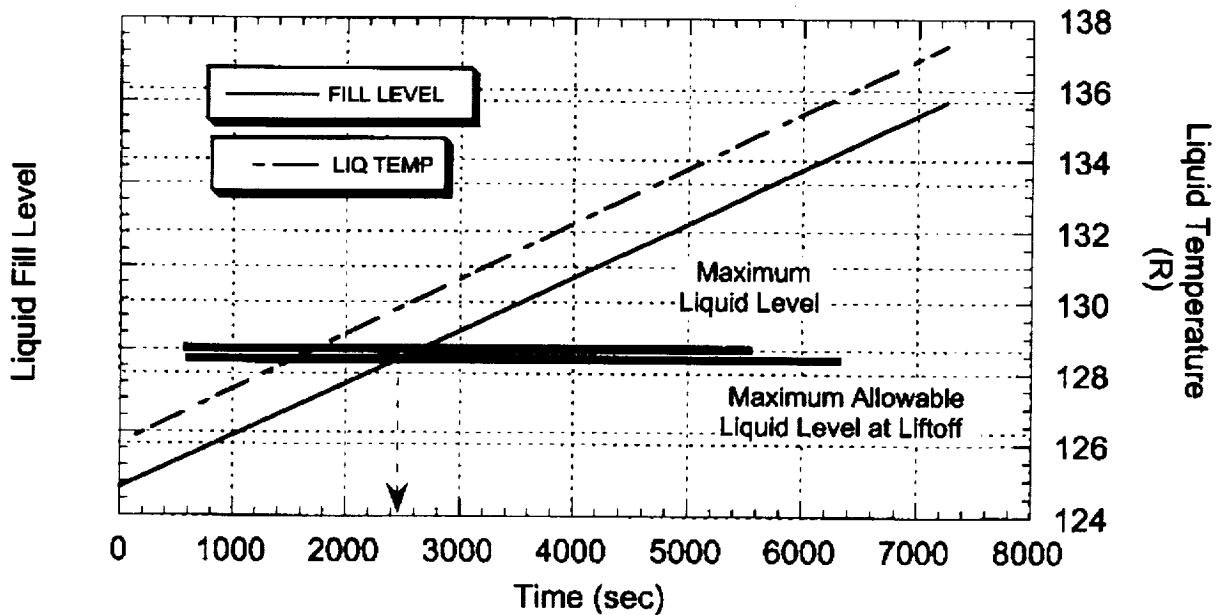


Figure 6.—Launch pad hold Centaur oxygen tank - densified oxygen at 126 R.

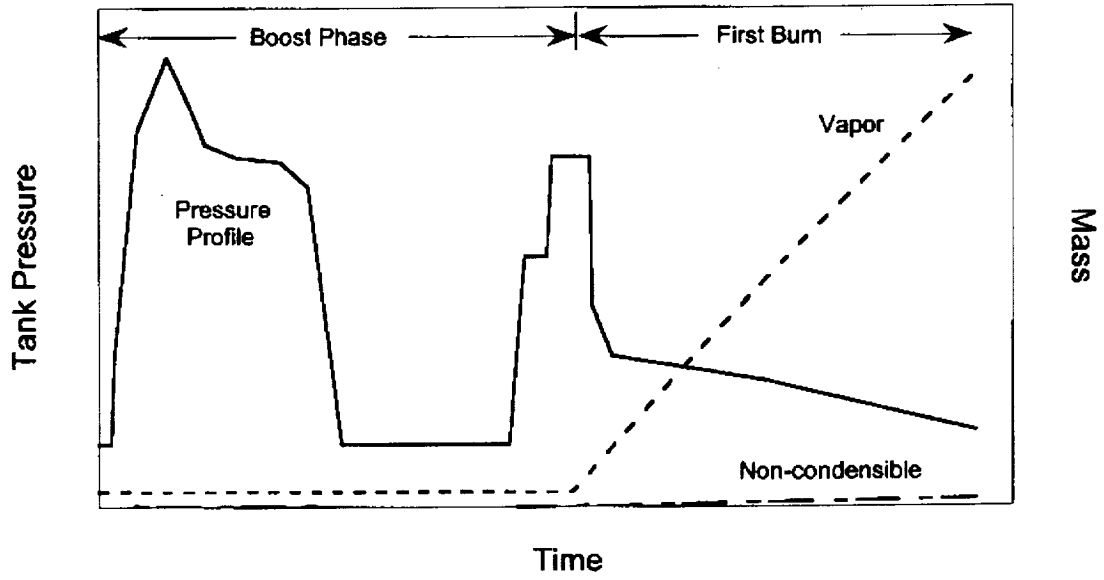


Figure 7.—Ullage mass Centaur oxygen tank - 176 R LOX.

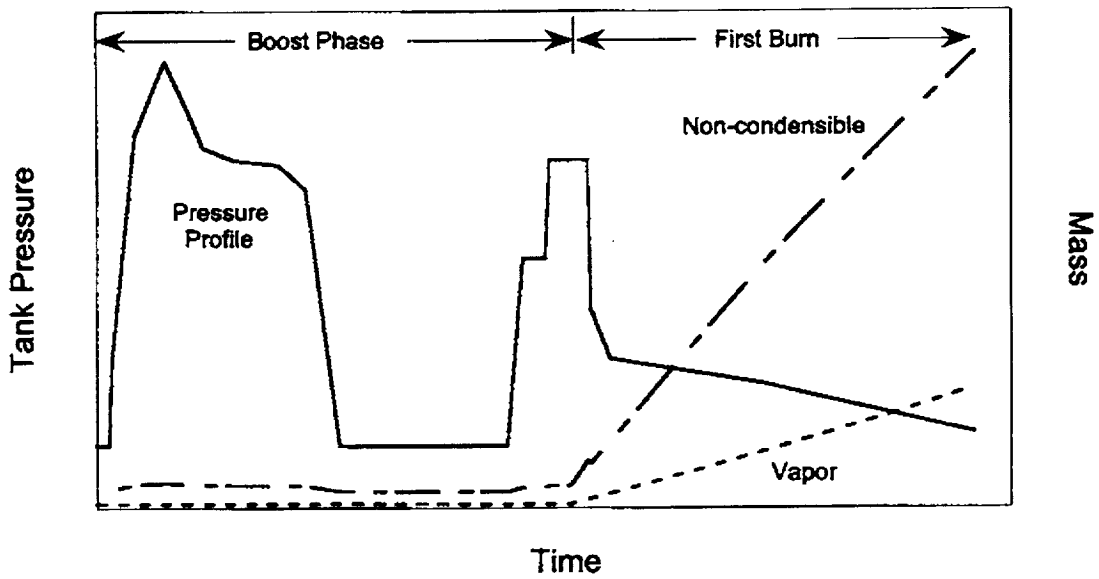


Figure 8.—Ullage mass Centaur oxygen tank - 126 R LOX.

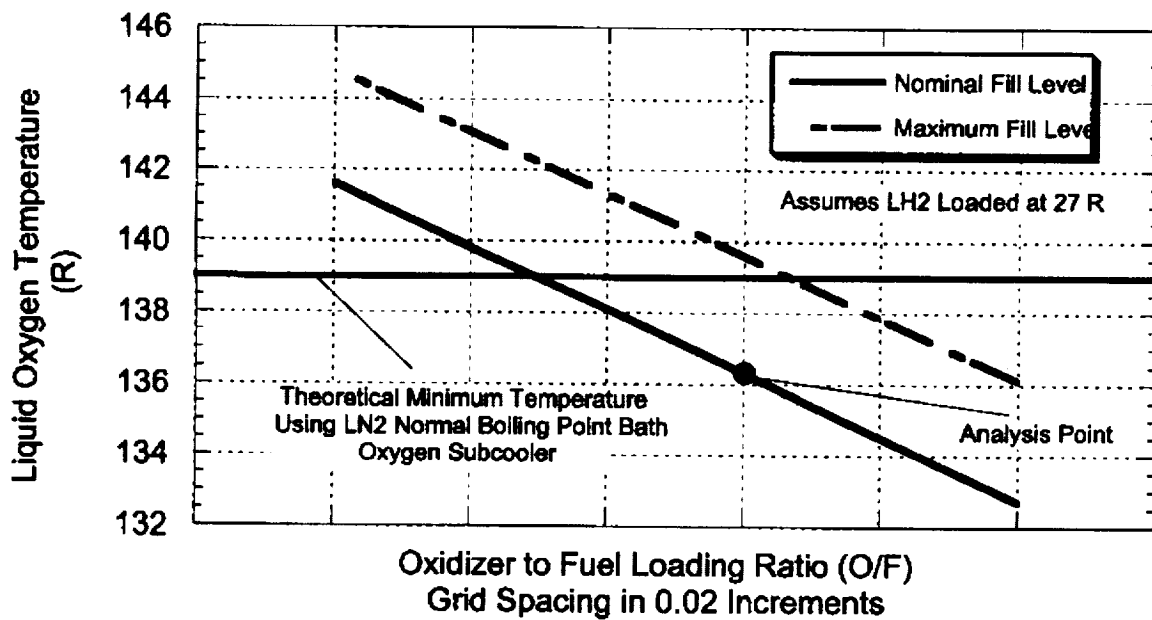


Figure 9.—Liquid oxygen temperature sensitivity to O/F loading ratio for fixed fuel mass.



# REPORT DOCUMENTATION PAGE

Form Approved  
OMB No. 0704-0188

Public reporting burden for this collection of information is estimated to average 1 hour per response, including the time for reviewing instructions, searching existing data sources, gathering and maintaining the data needed, and completing and reviewing the collection of information. Send comments regarding this burden estimate or any other aspect of this collection of information, including suggestions for reducing this burden, to Washington Headquarters Services, Directorate for Information Operations and Reports, 1215 Jefferson Davis Highway, Suite 1204, Arlington, VA 22202-4302, and to the Office of Management and Budget, Paperwork Reduction Project (0704-0188), Washington, DC 20503.

1. <b>AGENCY USE ONLY</b> ( <i>Leave blank</i> )	2. <b>REPORT DATE</b> April 2002	3. <b>REPORT TYPE AND DATES COVERED</b> Final Contractor Report	
4. <b>TITLE AND SUBTITLE</b>  Study Task for Determining the Effects of Boost-Phase Environments on Densified Propellants Thermal Conditions for Expendable Launch Vehicles		5. <b>FUNDING NUMBERS</b>  WU-721-20-00-00 NAS3-C-73676-J	
6. <b>AUTHOR(S)</b>  Mark S. Haberbusch		8. <b>PERFORMING ORGANIZATION REPORT NUMBER</b>  E-12715	
7. <b>PERFORMING ORGANIZATION NAME(S) AND ADDRESS(ES)</b>  Sierra Lobo, Inc. P.O. Box 250 Freemont, Ohio 43420		10. <b>SPONSORING/MONITORING AGENCY REPORT NUMBER</b>  NASA CR—2002-210808	
9. <b>SPONSORING/MONITORING AGENCY NAME(S) AND ADDRESS(ES)</b>  National Aeronautics and Space Administration Washington, DC 20546-0001		11. <b>SUPPLEMENTARY NOTES</b>  Project Manager, Michael L. Meyer, Turbomachinery and Propulsion System Division, NASA Glenn Research Center, organization code 5830, 216-977-7492.	
12a. <b>DISTRIBUTION/AVAILABILITY STATEMENT</b>  Unclassified - Unlimited Subject Categories: 15, 28, and 34 Available electronically at <a href="http://gltrs.grc.nasa.gov/GLTRS">http://gltrs.grc.nasa.gov/GLTRS</a> This publication is available from the NASA Center for AeroSpace Information, 301-621-0390.		12b. <b>DISTRIBUTION CODE</b>  Distribution: Nonstandard	
13. <b>ABSTRACT</b> ( <i>Maximum 200 words</i> )  A thermodynamic study has been conducted that investigated the effects of the boost-phase environment on densified propellant thermal conditions for expendable launch vehicles. Two thermodynamic models were developed and utilized to bound the expected thermodynamic conditions inside the cryogenic liquid hydrogen and oxygen propellant tanks of an Atlas IIAS/Centaur launch vehicle during the initial phases of flight. The ideal isentropic compression model was developed to predict minimum pressurant gas requirements. The thermal equilibrium model was developed to predict the maximum pressurant gas requirements. The models were modified to simulate the required flight tank pressure profiles through ramp pressurization, liquid expulsion, and tank venting. The transient parameters investigated were: liquid temperature, liquid level, and pressurant gas consumption. Several mission scenarios were analyzed using the thermodynamic models, and the results indicate that flying an Atlas IIAS launch vehicle with densified propellants is feasible and beneficial but may require some minor changes to the vehicle.			
14. <b>SUBJECT TERMS</b>  Densified propellants; Propellant; Rocket propellants; Pressurizing; Atlas Centaur launch vehicles; Centaur launch vehicle; Trajectory analysis			15. <b>NUMBER OF PAGES</b> 32
17. <b>SECURITY CLASSIFICATION OF REPORT</b> Unclassified			16. <b>PRICE CODE</b>
18. <b>SECURITY CLASSIFICATION OF THIS PAGE</b> Unclassified	19. <b>SECURITY CLASSIFICATION OF ABSTRACT</b> Unclassified	20. <b>LIMITATION OF ABSTRACT</b>	